

# Autophagic activity in cortical neurons under acute oxidative stress directly contributes to cell death

Gavin C. Higgins · Rodney J. Devenish ·  
Philip M. Beart · Phillip Nagley

Received: 4 October 2010 / Revised: 4 February 2011 / Accepted: 8 March 2011 / Published online: 25 March 2011  
© Springer Basel AG 2011

**Abstract** Primary neurons undergo insult-dependent programmed cell death. We examined autophagy as a process contributing to cell death in cortical neurons after treatment with either hydrogen peroxide ( $H_2O_2$ ) or staurosporine. Although caspase-9 activation and cleavage of procaspase-3 were significant following staurosporine treatment, neither was observed following  $H_2O_2$  treatment, indicating a non-apoptotic death. Autophagic activity increased rapidly with  $H_2O_2$ , but slowly with staurosporine, as quantified by processing of endogenous LC3. Autophagic induction by both stressors increased the abundance of fluorescent puncta formed by GFP-LC3, which could be blocked by 3-methyladenine. Significantly, such inhibition of autophagy blocked cell death induced by  $H_2O_2$  but not staurosporine. Suppression of Atg7 inhibited cell death by  $H_2O_2$ , but not staurosporine, whereas suppression of Beclin 1 prevented cell death by both treatments, suggesting it has a complex role regulating both apoptosis and autophagy. We conclude that autophagic mechanisms are activated in

an insult-dependent manner and that  $H_2O_2$  induces autophagic cell death.

**Keywords** Neurons · Oxidative stress · Programmed cell death · Autophagy · Caspases · LC3 · Atg7 · Beclin 1

## Abbreviations

3-MA	3-Methyladenine
DIC	Differential interference contrast
Endo G	Endonuclease G
GFP-LC3	Green fluorescent protein-tagged microtubule associated protein light chain 3
$H_2O_2$	Hydrogen peroxide
LC3	Microtubule associated protein light chain 3
nRNA	Non-specific RNA
PCD	Programmed cell death
PI	Propidium iodide
RFU	Relative fluorescence units
siAtg7	siRNA specific for <i>ATG7</i>
siBeclin1	siRNA specific for <i>BECN1</i>
STS	Staurosporine

G. C. Higgins · R. J. Devenish · P. Nagley (✉)  
Department of Biochemistry and Molecular Biology,  
Monash University, Building 13D, Clayton Campus,  
Clayton, VIC 3800, Australia  
e-mail: phillip.nagley@monash.edu

R. J. Devenish · P. Nagley  
Australian Research Council Centre of Excellence in Structural  
and Functional Microbial Genomics, Monash University,  
Clayton Campus, Clayton, VIC 3800, Australia

P. M. Beart  
Florey Neuroscience Institutes, University of Melbourne,  
Parkville, VIC 3010, Australia

P. M. Beart  
Department of Pharmacology, University of Melbourne,  
Parkville, VIC 3010, Australia

## Introduction

In post-mitotic neurons, autophagy is thought to be a critical process for the removal of damaged organelles and misfolded or aggregated proteins that are central to the pathophysiology of many neurodegenerative diseases. Much attention has recently been given to studying the potential inadequacy of autophagy in clearing dysfunctional mitochondria and toxic protein aggregates, such as  $\alpha$ -synuclein (Parkinson's disease), huntingtin (Huntington's

disease) and  $\beta$ -amyloid (Alzheimer's disease) during neurodegeneration [1–4]. Upregulation of autophagy has also been shown to occur in neuronal mice models of traumatic brain injury [5–7] and stroke [8–10].

Autophagy has also been identified as a programmed cell death (PCD) pathway under certain conditions, known as PCD-type II (where apoptosis is designated PCD-type I and programmed necrosis is PCD-type III) [11, 12]. The autophagic pathway most commonly associated with cell death is macroautophagy (hereafter referred to as “autophagy”), whereby organelles or molecules are sequestered within autophagosomes that are double membrane vesicles, which subsequently fuse with lysosomes leading to degradation of their cargo [1]. In response to cellular injury or disease, autophagy can be differentially recruited, either driving cellular homeostasis or inducing cell death, with the actual pattern of involvement likely dependent on energetics, load of cellular debris and/or insult nature [1–4]. To determine whether PCD-type II is invoked in these situations, it is essential to differentiate between these two opposing processes.

There have been several studies concerning neurons, which have implicated autophagy as a potential cell death mechanism, either by association (namely, observing autophagic activity during cell death) [13, 14] or through the use of autophagy inhibitors that arrest cell death [15, 16]. In order to strictly diagnose PCD-type II, one must first establish the occurrence of elevated autophagic activity, followed by demonstration that the induction of cell death explicitly depends on autophagic activity. The latter of these two steps can be carried out, in principle, with autophagic inhibitors such as 3-methyladenine (3-MA). However, because other cellular pathways are also the target of such autophagic inhibitors, it is more rigorous to apply genetic silencing via knockdown of the expression of key autophagy genes in order to confirm PCD-type II.

Oxidative stress is considered one of the principal instigators of cell death during many neuropathological conditions, including chronic diseases such as Alzheimer's disease and Parkinson's disease, as well as in more acute settings, such as during cerebral ischemic reperfusion following stroke [17–20]. In the stroke-affected brain, cell death has been considered to be necrotic at the center of the infarction and apoptotic in the penumbra surrounding the site of injury [21]. Apoptosis has previously been defined as a programmed or regulated type of cell death, characterized by the activation of caspases, while necrosis has been thought of as a caspase-independent, unregulated process. However, contemporary evidence supports the thesis that neuronal PCD is not exclusively apoptotic; rather it is a multifaceted phenomenon that encompasses autophagy and programmed necrosis, with extensive cross-talk between the three death pathways [22–24]. Within a

given population of neurons, it is thought that multiple PCD pathways can be invoked concurrently in response to a single injury or insult [25]. Thus, following stroke, caspase-independent cell death may not necessarily be unregulated necrosis, and there is for example recent evidence for the involvement of autophagy [8–10].

We previously established that, under oxidative stress induced by acute hydrogen peroxide ( $\text{H}_2\text{O}_2$ ) insult, PCD-type III is invoked in primary murine cortical neurons from C57 Black 6 J mice in the absence of caspase activity [26]. In this study, we set out to ascertain whether or not PCD-type II is also invoked under the same oxidative stress conditions. Staurosporine (STS), a widely used inducer of apoptosis [27], was used to aid the differentiation between PCD-type I and PCD-type II, as well as to help elucidate the role of autophagy in the cellular response to other stressors. Our data revealed a differential involvement of autophagy in neuronal injury, wherein cellular insults (both  $\text{H}_2\text{O}_2$  and STS) increased autophagic activity, although only cells treated with  $\text{H}_2\text{O}_2$  underwent PCD-type II.

## Materials and methods

### Cell culture

Primary cultures of murine neocortical neurons were established from embryonic day 15 C57/Black 6 J mice, as previously described [28, 29]. Cell densities were as follows: cell viability and confocal analyses ( $0.5 \times 10^5$  cells/well) and Western immunoblotting ( $2.5 \times 10^6$  cells/well). Under these conditions the cultures were essentially purely neuronal and contained <5% astrocytes [28, 29]. All experimentation received institutional ethical approval and was undertaken according to the Guidelines of the NH&MRC (Australia).

### Plasmid construction and transfection

pEGFP-LC3 was kindly provided by Dr. T. Yoshimori (National Institute of Genetics, Japan) [30]. Primary cortical neurons were transfected at 5 days in vitro [26]. Cells in a 24-well plate were transfected with 2  $\mu\text{g}$ /well of DNA and 6  $\mu\text{l}$ /well of Lipofectamine 2000 (1:3 ratio) in minimum essential medium with antioxidant-free B-27. Upon addition of the DNA/Lipofectamine 2000 mixture, cells were incubated for 4 h at 37°C to allow transfection to occur. Subsequently, the medium was replaced with Neurobasal medium<sup>TM</sup> containing complete B-27 (all the above media and transfection reagents were from Invitrogen, Melbourne, VIC, Australia). Under these conditions, typically 5% of neuronal cells were transfected with

GFP-LC3. Cells were then left to recover for 24 h before H<sub>2</sub>O<sub>2</sub> and STS treatments were performed.

#### Short interfering RNA (siRNA) transfections

Atg7 siRNA (Product Name: Mm\_Apg7l\_2\_HP Validated siRNA), Beclin 1 siRNA (product name, Mm\_Becn1\_3\_HP Validated siRNA) and negative control siRNA were purchased from Qiagen (Germantown, MD). Transfection of mouse primary cortical neurons with siRNA was carried out using HiPerFect transfection reagent (Qiagen, Doncaster, VIC, Australia) according to the protocols provided by the manufacturer. Under these conditions, typically 50–70% of neuronal cells were transfected by control siRNA. Transfections were carried out as previously described [26].

#### Drug exposure

Guided by our previous work [29, 31], neuronal cultures were exposed to either 50  $\mu$ mol/l H<sub>2</sub>O<sub>2</sub> [30% (w/v), Merck, Melbourne, VIC, Australia] or 200 nmol/l STS (Sigma-Aldrich, Castle Hill, NSW, Australia) in Minimum Essential medium with antioxidant-free B-27 (Invitrogen, Melbourne, VIC, Australia). In some experiments, treatment of neurons with STS or H<sub>2</sub>O<sub>2</sub> was also performed in the presence of a broad spectrum caspase inhibitor z-Val-Ala-Asp(OCH<sub>3</sub>)-CH<sub>2</sub>F (zVAD-fmk) (Bachem, Bubendorf, Switzerland) at 100  $\mu$ mol/l. Cells were pre-treated with zVAD-fmk in Minimum Essential medium with antioxidant-free B-27, 30 min prior to treatment with STS or H<sub>2</sub>O<sub>2</sub>, with zVAD-fmk remaining in the medium during such subsequent treatments. Some neurons were also pre-treated with the autophagy inhibitor 3-methyladenine (3-MA) (Sigma-Aldrich, Castle Hill, NSW, Australia) at 10 mmol/l for 30 min prior to treatment with 50  $\mu$ mol/l H<sub>2</sub>O<sub>2</sub> (30% (w/v), Merck, Melbourne, VIC, Australia) or STS (200 nmol/l, Sigma-Aldrich, Castle Hill, NSW, Australia).

#### Cell viability

Cells from cultures were directly stained with 5  $\mu$ g/ml of propidium iodide (PI) (Invitrogen Molecular Probes, Melbourne, VIC, Australia) in 1 $\times$  phosphate buffered saline, pH 7.4 (PBS). Following incubation for 5 min at 37°C, cells stained with PI were washed three times with 1 $\times$  PBS before being fixed with 3% paraformaldehyde in 1 $\times$  PBS at 22°C, and then mounted on glass slides [29, 32].

#### Nuclear morphology

Staining of nuclei with 4',6-diamidino-2-phenylindole (DAPI) (Invitrogen Molecular Probes, Melbourne, VIC,

Australia) was carried out as described [29], and the morphology determined by confocal microscopy (see below).

#### Immunocytochemistry

Immunocytochemistry was performed as described [32]. In this work, following fixation and permeabilization, samples were then incubated for 3 h at 22°C with rabbit polyclonal anti-cleaved caspase-9 (1:100, Calbiochem, Kilsyth, VIC, Australia). Following incubation with the primary antibody, samples were processed as described [32]. The secondary antibody used was Alexa568-labeled goat anti-rabbit IgG (1:200, Invitrogen Molecular Probes, Melbourne, VIC, Australia).

#### Confocal microscopy

Samples were imaged by fluorescence laser scanning confocal microscopy using an Olympus FluoView 500, IX81 inverted confocal microscope (Olympus, Melbourne, VIC, Australia), fitted with a UPlan Apo 60 $\times$ /1.20w water immersion lens. Images were captured using Fluroview software (Olympus, Melbourne, VIC, Australia). In multiple fluorescence channel imaging, photomultiplier sensitivities, gain levels and offsets were adjusted to ensure that there was little or no bleed-through of fluorescence signal from one channel to the other. A Kalman filter was used to reduce background noise levels. The selected field was scanned five times using a “Frame Kalman” scan. All fields were scanned sequentially in order to reduce the incidence of ‘bleed through’ between each of the channels used. Three hundred cells were scored for each population scored, and three independent experiments were undertaken for each condition tested. Image Tool Software version 3.00 (developed by the Department of Dental Diagnostic Science at The University of Texas Health Science Center, San Antonio, TX) was used to assist the manual scoring of cellular morphologies.

#### Western immunoblotting

Following treatment with H<sub>2</sub>O<sub>2</sub> and STS, cells were harvested by gentle scraping and centrifugation (800g, 5 min), and treated with RIPA extraction buffer (10 mM Tris-HCl pH 8.0, 150 mM NaCl, 1% NP-40, 1% sodium deoxycholate, 0.1% SDS; protease inhibitor cocktail) (Sigma-Aldrich, Castle Hill, NSW, Australia) for 5 min at 4°C. The supernatant obtained by centrifugation (15,000g, 15 min) at 4°C was retained for western immunoblot analyses. The protein concentration of supernatants was determined using a BCA Protein Assay Kit (Pierce, Rockford, IL). The proteins were denatured in Laemmli sample buffer (Bio-Rad, Hercules, CA) at 95°C for 5 min,

and separation was carried out on a 12% NuPAGE Bis-Tris pre-cast gel (Invitrogen, Melbourne, VIC, Australia) where the protein ladder (10  $\mu$ l) and sample (20  $\mu$ l, 15–20  $\mu$ g total protein) were separated at 200 V for 30 min. Routine procedures were used for transfer, washing, blocking and probing of blots. Membranes were incubated overnight at 4°C with either primary rabbit polyclonal anti-caspase-3 antibody (1:1,000) or anti-caspase-7 antibody (1:500) (both from Cell Signaling, Danvers, MA); rabbit polyclonal anti-LC3 antibody (1:1,000, Novus Biologicals, Littleton, CO); rabbit polyclonal anti-Atg7 or Beclin 1 antibodies (1:1,000, Pro-Sci Inc, Poway, CA); or mouse monoclonal anti- $\beta$ -actin antibody (1:400, Neomarkers, Fremont, CA). The appropriate secondary species-specific (anti-rabbit or anti-mouse) Alexa488-labeled goat anti-IgG antibody (1:1,000; Invitrogen-Molecular Probes, Melbourne, VIC, Australia) was incubated for 2 h at room temperature. Precision Plus Protein<sup>TM</sup> (Bio Rad, Gladsville, NSW, Australia) and SeeBlue<sup>®</sup> Plus2 (Invitrogen, Melbourne, VIC, Australia) molecular weight standards were used to reference molecular weights in Western immunoblots. Densitometry was performed as described previously [26].

#### Caspase-9 fluorescence activity assays

Caspase-9 activity was measured directly by examining the cleavage of an AFC-LEHD substrate (Calbiochem, Kilsyth, VIC, Australia) by active caspase-9 in cell lysates. Neurons were cultured in 24-well plates ( $0.5 \times 10^6$  cells/well) and processed according to the manufacturer's instructions. In brief, after exposure to the desired insult, cells were lysed in situ and the lysates collected into 96-well microtiter plates for the fluorescence assay of caspase-9 activity, based on fluorescence shift of AFC-LEHD substrate after cleavage of the peptide moiety. Fluorescence was expressed in relative fluorescence units (RFU) (excitation 390 nm/emission 510 nm), following measurements in a Fluorostar Optima plate reader (BMG Labtech, Mornington, VIC, Australia).

#### Statistical analysis

Comparative data sets were analyzed using one- and two-way ANOVA, followed by Bonferroni's post hoc test. One-way ANOVA was used for intra-group analysis, while two-way ANOVA was carried out to compare populations subjected to different treatments. Data from Western immunoblotting were analyzed by non-parametric ANOVA with Dunn's post hoc test (GraphPad Prism, San Diego, CA). The results are expressed as the mean  $\pm$  SEM. Unless otherwise indicated, data are from three independent experiments with replicate determinations

( $n = 3$ –5). The differences were considered significant at  $p < 0.05$ .

## Results

### Effector caspases-3 and caspase-7 are not cleaved following treatment with H<sub>2</sub>O<sub>2</sub>

Cleavage of caspase-3 and caspase-7 was studied by performing Western immunoblots on lysates collected from neurons treated with moderate doses of either H<sub>2</sub>O<sub>2</sub> (50  $\mu$ mol/l) or STS (200 nmol/l). At higher doses, cells became necrotic in the case of H<sub>2</sub>O<sub>2</sub> and progressed through PCD too rapidly for effective analysis (data not shown). We have previously demonstrated [26] the barely detectable activation of caspase-3 and caspase-7 in neurons after H<sub>2</sub>O<sub>2</sub> insult, as determined by activity measurements using the fluorescent substrate FITC-DEVD-fmk (for caspase-3 as a direct assay and for caspase-7 as a specific fluoregenic/immunoassay). Further, after STS insult caspase-3 was significantly activated, but not caspase-7 [26]. However, it remained unclear whether the very low caspase activity observed after H<sub>2</sub>O<sub>2</sub> treatment was due to a substantial failure of caspase cleavage, as such. Western immunoblots probed with anti-caspase-3 antibody showed an increase of cleaved caspase-3 over 24 h after STS treatment (Fig. 1a). By contrast, H<sub>2</sub>O<sub>2</sub> treatment resulted in very little detectable cleaved caspase-3 after 24 h (Fig. 1a).

Western immunoblots probed with anti-caspase-7 antibody showed procaspase-7 was not cleaved after treatment with either STS or H<sub>2</sub>O<sub>2</sub> (Fig. 1b). As we showed previously [26], caspase-7 is not activated after STS treatment of these neurons. To better understand these activities for downstream caspases, a study of caspase-9 activation, which occurs upstream of caspase-3 and caspase-7 activation, was made.

### Initiator caspase-9 is not activated following treatment with H<sub>2</sub>O<sub>2</sub>

The activation of initiator caspase-9 was analyzed under cellular oxidative insult. Immunocytochemical staining for active caspase-9 (in this case cleaved pro-caspase-9) (Fig. 2a) showed levels of active caspase-9 to rise slightly over time during STS treatment, although changes in cleaved pro-caspase 9 were not significant over this 24-h period (Fig. 2b). However, it should be noted that it is not necessary for pro-caspase-9 to be cleaved to become active [33], which may also explain the relatively low levels of cleaved pro-caspase-9 seen in the STS-treated neurons. Caspase-9 activity measurements using AFC-LEHD

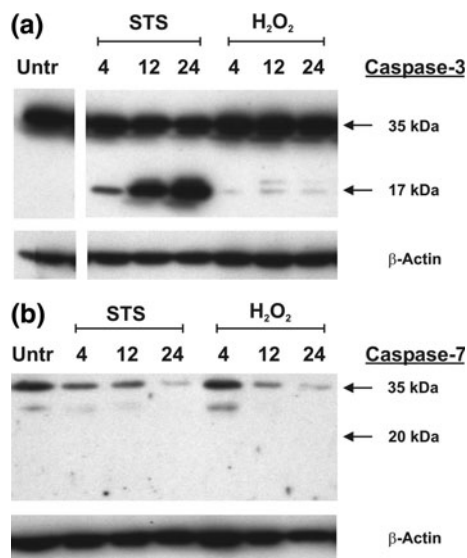


**Fig. 1** Caspase-3 and caspase-7 cleavage during treatment of primary cortical neurons with STS or  $H_2O_2$ . **a** Western immunoblot of caspase-3 in cell lysates;  $\beta$ -actin is shown as loading control. Lanes indicate untreated control (Untr), and cells treated with either STS or  $H_2O_2$  for different times (4, 12, 24 h). Positions on gel of pro-caspase-3 (35 kDa) and cleaved caspase-3 (17 kDa) are shown at right (determined with reference to protein markers of different molecular weights, not shown here). **b** Western immunoblot of caspase-7 in cell lysates, with  $\beta$ -actin as loading control. Lanes are indicated as for caspase-3 immunoblot shown above. Positions of pro-caspase-7 (35 kDa) and cleaved (20 kDa) are shown at right

substrate indicate that activation of this enzyme occurs in STS-treated neurons, but not in those treated with  $H_2O_2$  (Fig. 2c). Significantly, this assay also showed that caspase-9 activation induced by STS is strongly inhibited by the pan-caspase inhibitor z-VAD-fmk, confirming that these cultured cortical neurons are indeed capable of activating caspase-9.

These cortical neurons fail to activate caspase-9 following  $H_2O_2$  treatment, which may explain the lack of subsequent activation of downstream caspase-3 and caspase-7. The lack of caspase activity after  $H_2O_2$  insult confirms that the type of cell death that occurs in these cells under acute oxidative stress is caspase-independent.

Autophagic activity is elevated in neurons treated with either STS or  $H_2O_2$

Microtubule-associated light chain 3 (LC3) is recruited during the early expansion of isolation membranes and persists until the completed autophagosomes fuse with the lysosome [34, 35]. Here autophagy was monitored by utilizing LC3 fused to green fluorescent protein (GFP-LC3) to visualize autophagic activity by confocal microscopy, in concert with Western immunoblotting to monitor conversion of LC3-I to LC3-II (resulting from a conformational

modification during vesicle formation) to quantify fluxes in autophagic activity [34, 35]. The autophagy pathway was inhibited both pharmacologically through the use of 3-MA and through knockdown of the autophagy proteins Atg7 and Beclin 1.

Autophagic activity was initially monitored by quantifying the conversion of LC3-I to LC3-II, which occurs during autophagic vesicle formation. Changes in LC3-II levels over time were determined by quantifying LC3-II relative to  $\beta$ -actin using densitometry. LC3-II levels increased rapidly following  $H_2O_2$  treatment (Fig. 3a), almost doubling after 4 h and increasing rapidly in a time-dependent manner, being threefold by 24 h, relative to the control (Fig. 3c). Similarly, LC3-II levels doubled at 4 h relative to the control, and continued to increase up to 12 h with STS (Fig. 3b, d). These results indicated that autophagic activity increased differentially in response to both cellular insults, being activated by both  $H_2O_2$  and STS.

Single cell analysis of neurons transfected with GFP-LC3 was also undertaken to determine the proportion of the neuronal population that shows an increase in autophagic activity. Neurons were determined to have an increase in autophagic activity when there was an increase in GFP-LC3 recruited to autophagic vesicles as represented by fluorescent green puncta within the cells. In untreated neurons the fluorescence of GFP-LC3 was seen to be diffuse throughout the cytosol of the cell body and axon (Fig. 4, first image on left, in each of a and b). In neurons treated with either  $H_2O_2$  or STS, GFP-LC3 was localized into autophagic puncta (Fig. 4, second image top right, in each of a and b). As there was always a basal level of autophagy occurring within neurons to help maintain cellular homeostasis, we set a minimal threshold of five observed puncta per cell to define cells displaying autophagic activity. Cells displaying <5 puncta were determined to be at a basal level of autophagy.

Quantification of GFP-LC3 transfected neurons revealed that autophagic activity increased in 40% of the total population of neurons after 24 h treatment with  $H_2O_2$  (Fig. 4c). Similarly, 40% of transfected neurons treated with STS had elevated autophagic activity after 24 h relative to the untreated control (Fig. 4d). To verify that the observed puncta were autophagic vesicles, neurons were pre-treated with autophagy inhibitor 3-MA to arrest puncta formation (Fig. 4, third image bottom right, in each of a and b). Transfected neurons pre-treated with 3-MA, followed by either  $H_2O_2$  or STS, had reduced autophagic activity (Fig. 4, c, d), with the number of neurons displaying elevated puncta formation returning to levels close to those in untreated cell populations. Neurons were also pre-treated with the pan-caspase inhibitor z-VAD-fmk to establish whether classical apoptosis (caspase-dependent) was involved in the activation of autophagy. Pre-treatment with z-VAD-fmk had no effect on autophagic activity in



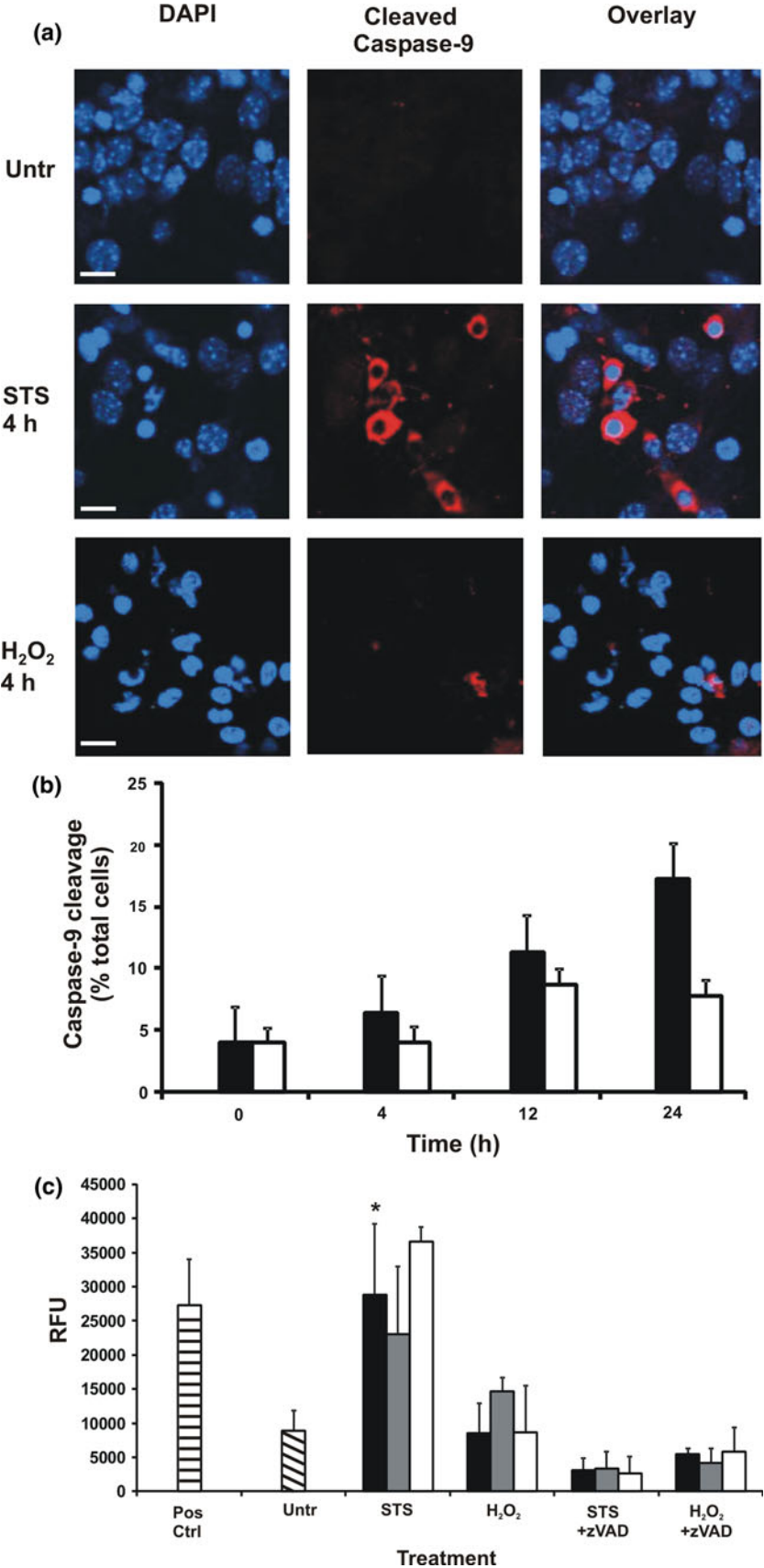


**Fig. 2** Caspase-9 activation during STS and H<sub>2</sub>O<sub>2</sub> treatment. **a** Antibody specific for activated caspase-9 was used to stain neurons immunochemically. DAPI was used as a counterstain for nuclei to determine the total number of cells per field. Images are shown for untreated (Untr) neurons and those treated with STS or H<sub>2</sub>O<sub>2</sub> for 4 h. Treatments were as described in the text. Note that the discernable frequency of condensed nuclei in untreated cultures (up to 20%) reflects the spontaneous death rate in these primary neuronal cultures as seen with PI uptake (e.g., Figs. 5b, 6c). Bars represent 10  $\mu$ m. **b** Quantitative analysis of treated populations. Black bars, STS; white bars, H<sub>2</sub>O<sub>2</sub>. Data for each population scored represent the mean percentage of cells scored for caspase-9 activation ( $n = 300$ –500 for each population). Values are mean  $\pm$  SEM of three independent experiments. **c** Caspase-9 activity measured by fluorescence of cleaved substrate analog AFC-LEHD. Neurons were treated with STS or H<sub>2</sub>O<sub>2</sub> in 24-well plates for various times; in some populations zVAD-fmk (indicated by +zVAD) was additionally included during the treatment. Following treatment, cell lysates were generated and then collected for caspase-9 activity tests. Horizontally striped bar, positive control (Pos Ctrl) corresponding to recombinant caspase-9 incubated with AFC-LEHD; diagonally striped bar, untreated (Untr); black bars, 4 h; gray bars, 12 h; white bars, 24 h. Fluorescence intensities are indicated as relative fluorescence units (RFU). Asterisk indicates the earliest time point for a given feature that displays significant difference ( $P < 0.05$ ) comparing a treated population with the relevant untreated control. Data for each treatment condition and time represent the mean  $\pm$  SEM of three independent experiments, each carried out in triplicate wells on a single microtiter plate

neurons treated with either H<sub>2</sub>O<sub>2</sub> or STS, indicating that autophagy activation under both conditions was independent of any caspase activity (Fig. 4c, d).

#### PCD-Type II contributes to H<sub>2</sub>O<sub>2</sub>-induced cell death

Cell death was determined by scoring neurons that were permeable to PI (Fig. 5a). This test indicates the compromised integrity of the plasma membrane, but is not a strict marker, as such, for distinguishing necrosis and apoptosis [12]. Note that, as in our previous study on primary cortical neurons [26], about 10–20% of cells otherwise untreated show PI uptake. For neurons treated with H<sub>2</sub>O<sub>2</sub> approximately 60% of cells were positive for PI uptake after 24 h (Fig. 5b). The extent of PI permeability was reduced to approximately 35% when neurons were pretreated with 3-MA (Fig. 5b). Pre-treatment of neurons with z-VAD-fmk had no effect, as anticipated, because of the lack of caspase-3 and caspase-7 cleavage seen under these conditions (Fig. 5b). On the other hand, for neurons exposed to STS, ~60% of cells were PI-positive after 24 h (Fig. 5c). However, unlike neurons treated with H<sub>2</sub>O<sub>2</sub>, pretreatment with 3-MA of STS treated neurons had no effect on prevention of cell death. Pretreatment with z-VAD-fmk also had no effect in preventing cell death (Fig. 5c), an outcome that could be attributable to alternative caspase-independent cell death pathways being invoked [26] or the commitment to demise being insensitive to downstream caspase inhibition [22].

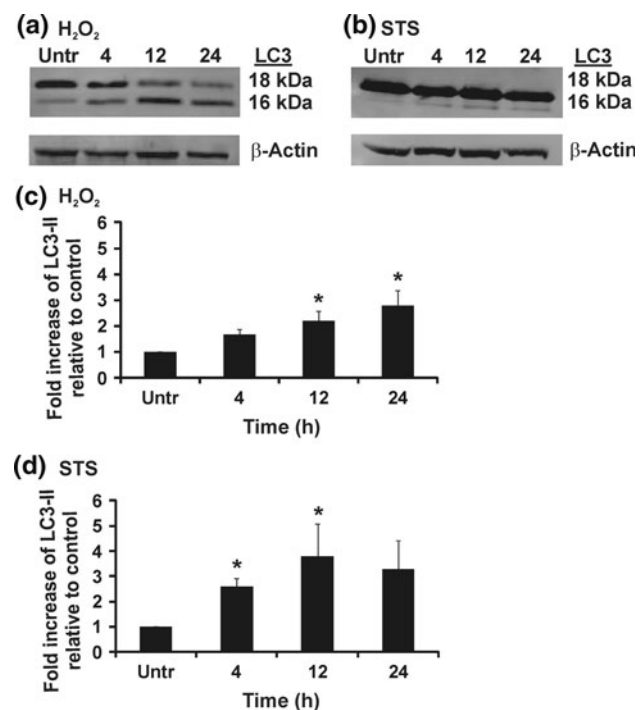


**Fig. 3** Conversion of LC3-I to LC3-II in cell lysates from primary cortical neurons treated with either H<sub>2</sub>O<sub>2</sub> or STS. **a** Western immunoblot of LC3 in cell lysates isolated from neurons treated with H<sub>2</sub>O<sub>2</sub>;  $\beta$ -actin is shown as a loading control. Lanes indicate untreated (Untr) neurons and those treated with H<sub>2</sub>O<sub>2</sub> at various times (4, 12, 24 h). Positions on the gel of LC3-I (18 kDa) and LC3-II (16 kDa) are shown at right. **b** Western immunoblot of LC3 in cell lysates isolated from neurons treated with STS. All indications are the same as in **a**. **c** Quantitative analysis of fold increase of LC3-II relative to  $\beta$ -actin. Overall changes ( $P < 0.01$ ) with individual changes ( $*P < 0.05$ ) shown. **d** Quantitative analysis of fold increase of LC3-II relative to  $\beta$ -actin. Overall changes ( $P < 0.05$ ) with individual changes ( $*P < 0.05$ ) shown. The fold increase of LC3-II shown in the histograms of **c** and **d** is for the exemplar immunoblots shown in **a** and **b**; it represents a very similar relationship obtained from three independent experiments (not shown)

#### Knockdown of Atg7 suppresses cell death in cortical neurons during H<sub>2</sub>O<sub>2</sub> treatment

The formation of the conjugated form of LC3 (LC3-II) is dependent on Atg7 [36]. Given the lack of specificity of pharmacological inhibitors of autophagy [37], we further investigated the dependence on autophagic machinery using siRNA specific for ATG7 (siAtg7) to knock down expression of Atg7. While non-specific RNA (nRNA) induced little or no change in cellular Atg7 levels, with siAtg7 knockdown of Atg7 expression greater than 60% was routinely achieved (Fig. 6a). Individual replicate experiments all showed knockdown in the range of 60–80% (data not shown). Neurons transfected with siAtg7 or nRNA were then treated with H<sub>2</sub>O<sub>2</sub> or STS, and monitored for changes in nuclear morphology and cell death (Fig. 6b). Cell death induced by H<sub>2</sub>O<sub>2</sub> was reduced in

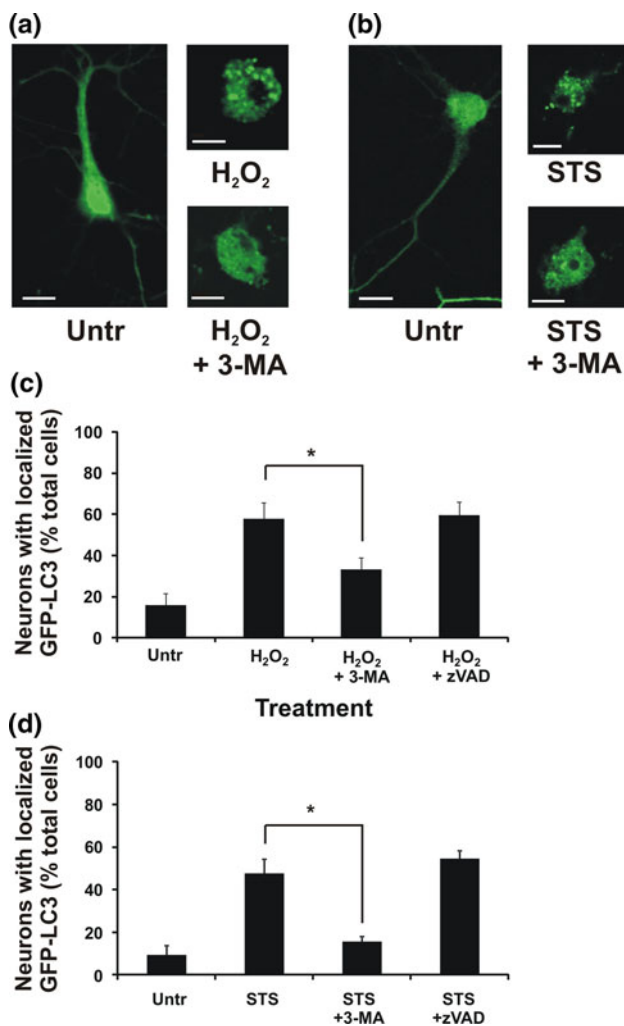


**Fig. 4** Mobilization of GFP-LC3 from cytosol to autophagic vesicles in primary cortical neurons treated with  $H_2O_2$  or STS. **a** Neurons transfected with GFP-LC3, subsequently treated with  $H_2O_2$ . Images represent: untreated (Untr);  $H_2O_2$  treatment; 3-MA treatment prior to addition of  $H_2O_2$ . Images were taken with a  $\times 60$  optical magnification, with suitable electronic zoom to enable optimal visualization of autophagic puncta. Bars represent 10  $\mu m$ . **b** Neurons transfected with GFP-LC3, subsequently treated with STS. Images are otherwise indicated as in **a**. **c, d** Quantitative analysis of neurons scored for localization of GFP-LC3 into puncta. Neurons scored as “localized GFP-LC3” were identified by having a minimum of five fluorescent puncta observed within a single cell. Data for each population thus scored were determined as the mean percentage of cells with this morphology ( $n = 100$  for each population). Values shown in histogram are mean  $\pm$  SEM of three independent experiments. Asterisks indicate a significant difference ( $P < 0.05$ ) in the mean percentage of neurons scored with localized GFP-LC3, comparing treated populations with or without 3-MA

neurons transfected with siAtg7, but not nRNA (Fig. 6 b, c). Conversely, STS-induced cell death was not inhibited following transfection with either siAtg7 or nRNA (Fig. 6 b, c). These findings concurred with inhibition of cell death observed in the presence of 3-MA, suggesting

that autophagy as such, or key components of the autophagy pathway, are not involved in the death of these neurons.

In transfected neurons treated with either STS or  $H_2O_2$ , nuclear morphology was studied as another index of cell death. Nuclei were observed to become condensed in  $H_2O_2$ -treated neurons and fragmented in STS-treated neurons, respectively (Fig. 7a). Transfection with siAtg7 slowed the pattern of changes in morphology such that the number of condensed nuclei was reduced at 4 h ( $\sim 30\%$ ) relative to the nRNA population for  $H_2O_2$ , but not at later time points (Fig. 7b). However, for STS, siAtg7 failed to affect the number of modified nuclei at all time points. We further reason that nuclear modification occurs before loss of plasma membrane integrity during PCD, thus knock-down of Atg7 has only delayed  $H_2O_2$ -induced cell death rather than completely suppressed it.

#### Knockdown of Beclin 1 suppresses $H_2O_2$ and STS-induced death

Another key autophagic protein, Beclin 1, located upstream of Atg7 in the autophagy pathway, was also studied because of its potential as a mediator between the autophagic and apoptotic pathways [38, 39]. Expression of *BECN1* was knocked down using siRNA (siBeclin 1), with knockdown of approximately 60–90% being routinely achieved (Fig. 8a). Cell death was suppressed in siBeclin 1-transfected neurons treated with either  $H_2O_2$  or STS (Fig. 8b). Moreover, silencing of Beclin 1 suppressed nuclear morphology changes in  $H_2O_2$ -treated neurons, but not in those treated with STS (Fig. 8c). These findings, after Beclin 1 suppression, confirm that autophagy as such has a direct role in cell death induced by  $H_2O_2$  (as seen with Atg7 suppression and 3-MA inhibition). In contrast, the situation in STS-treated cells under Beclin 1 suppression is not so clear, as blockade of autophagy was not expected to suppress cell death.

Moreover, silencing of Beclin 1 suppressed nuclear morphology changes in  $H_2O_2$ -treated neurons (as expected), but not in those treated with STS (Fig. 8c). It is therefore evident that Beclin 1 has a more complex role in both autophagy and cell death (including apoptosis) induced by STS, as considered below.

#### Discussion

This investigation employed various cellular and molecular approaches to dissect the pattern of involvement of autophagic mechanisms in neuronal injury [37]. Autophagy has been much studied in the neurobiological context as a process recruited because of the cellular presence of



potentially cytotoxic misfolded proteins, especially  $\alpha$ -synuclein,  $\beta$ -amyloid and huntingtin, which potentially threaten neuronal survival in pathological conditions [4, 40]. However, in the context of our novel findings on the patterns of involvement of autophagy in neuronal injury, it is timely to recall that autophagy is an adaptive and multifaceted process by which cells handle bioenergetic crises,

and which can be both cytoprotective and destructive [2, 3]. A key finding of our work is that autophagic mechanisms are activated in an insult-dependent manner during neuronal injury and that the pattern of involvement is different not only from a temporal perspective, but importantly from a cell death perspective. While we found that Beclin 1 is recruited to cell death involving both

**Fig. 5** Cell death in primary cortical neurons induced by  $H_2O_2$  or STS. Some neurons were also pre-treated with 3-MA (or zVAD) as indicated. Neurons were treated for 24 h with stressors  $H_2O_2$  or STS, at which time the extent of uptake of PI into individual cells was determined. **a** Upper row shows images of cells stained with PI. The second row shows DIC imaging, in order to visualize the total number of cells within the same field. Images are shown for untreated (Untr) neurons and those treated with  $H_2O_2$  or STS, and 3-MA, where indicated. Bars represent 10  $\mu$ m. **b** Quantitative analysis of PI uptake under  $H_2O_2$  treatment. Data for each population scored represent the mean percentage of cells scored for PI uptake ( $n = 100$  for each population). Values shown in the histogram are mean  $\pm$  SEM of three independent experiments. Asterisks indicate a significant difference ( $P < 0.05$ ) in cell death, comparing treated populations with and without 3-MA. **c** Quantitative analysis of PI uptake under STS treatment. Indications as in **b**

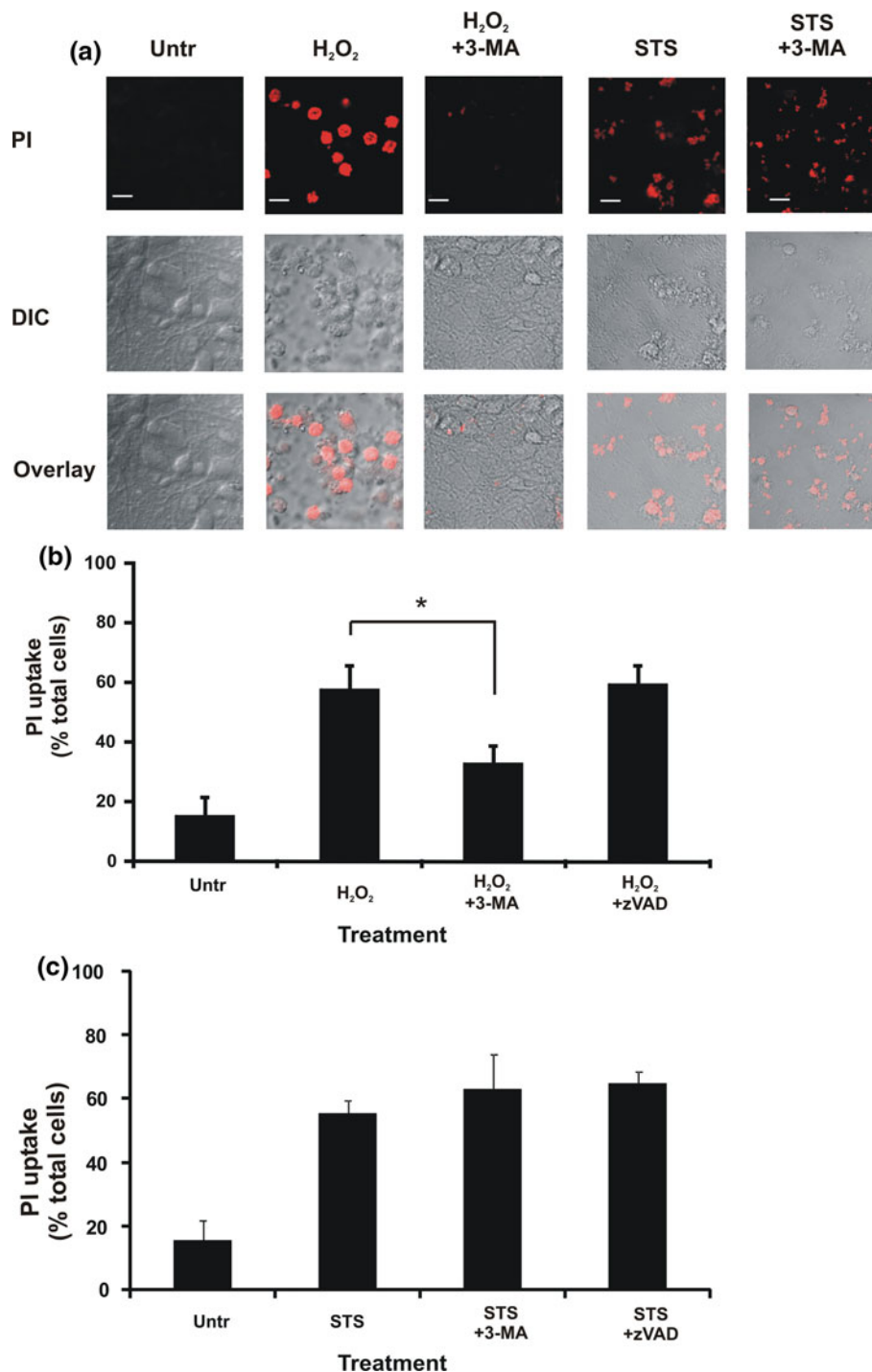
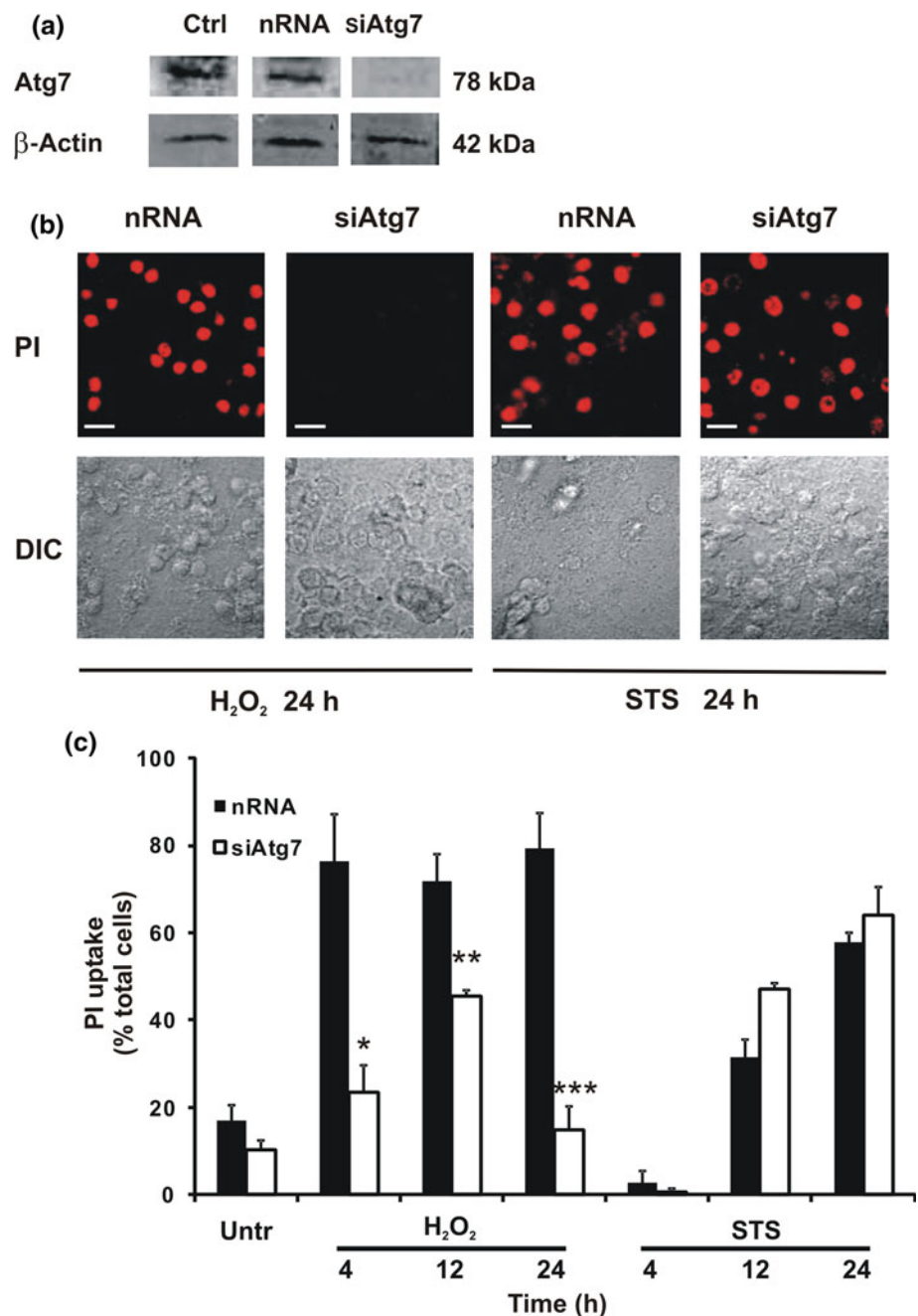


**Fig. 6** Cell death in  $H_2O_2$ -treated and STS-treated primary cortical neurons transfected with nRNA or siAtg7.

**a** Western immunoblots of Atg7 in cell lysates;  $\beta$ -actin is shown as loading control. *Lanes* indicate untransfected control (Ctrl), and cells transfected with nRNA or siAtg7. Sizes of proteins visualized (kDa) are indicated at *right*. Representative gel shown here indicates >80% suppression of Atg7 expression by siAtg7.

**b** Images of PI uptake in transfected cortical neurons after treatment with either  $H_2O_2$  or STS for 24 h. DIC images are provided to visualize the total number of cells in each field. Bars represent 10  $\mu$ m.

**c** Quantitative analysis of PI uptake in transfected cells after treatment with  $H_2O_2$  or STS. Results shown here report triplicate analyses within a single experiment ( $n = 100$  for each population). Due to the variation in the Atg7 suppression achieved between different transfection experiments using siRNA (see text), similar data obtained from three replicate experiments were not combined for quantification here. Asterisks indicate time points where there was a significant difference between nRNA and siAtg7 populations (\* $P < 0.001$ , \*\* $P < 0.01$ , \*\*\* $P < 0.001$ )



PCD-type I and -type II, the mode of involvement of the autophagy process itself is not always destructive in relation to cell death.

$H_2O_2$ -treated neurons displayed autophagic cell death, in that caspase activity was absent, and cell death was found to be directly dependent on both Beclin 1 and Atg7, and was inhibited by 3-MA (Fig. 9). Thus, the autophagic pathway is activated as PCD-type II, apparently to expedite elimination of non-viable neurons. Conversely, STS-treated neurons were shown to be apoptotic with caspase

activation. While the autophagic pathway was activated by STS, it was shown not to contribute to cell death (Fig. 9) (discussed in more detail below). This finding suggested that the autophagic pathway is recruited in a cytoprotective manner in response to STS treatment. However, STS was also shown to have a dependence on Beclin 1 recruitment for inducing cell death. This finding indicated that Beclin 1 may in fact have dual roles, acting in both apoptosis and autophagy, as has been recently reported by others [41].

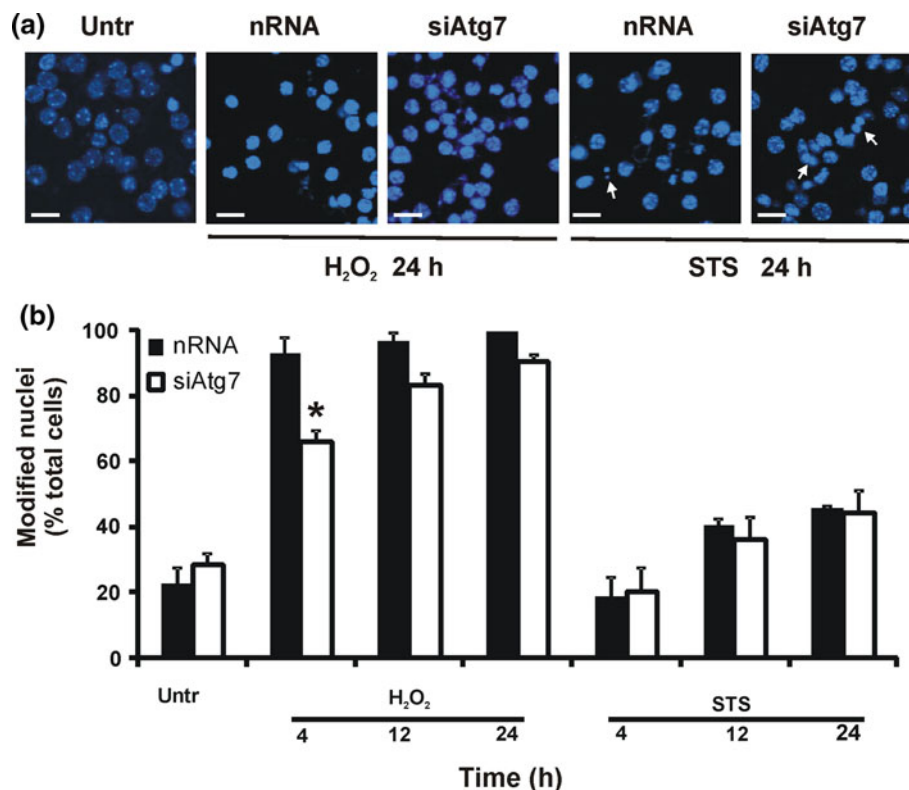


**Fig. 7** Changes in nuclear morphology in H<sub>2</sub>O<sub>2</sub>-treated and STS-treated primary cortical neurons transfected with nRNA or siAtg7. **a** Nuclear morphology revealed by DAPI staining of neurons after STS or H<sub>2</sub>O<sub>2</sub> treatment for 24 h. Images are shown for untreated (Untr) neurons and those treated with either H<sub>2</sub>O<sub>2</sub> or STS. Neurons transfected with nRNA show the same features as for those treated with stressors but not transfected (data not shown). Nearly all nuclei were condensed after H<sub>2</sub>O<sub>2</sub> treatment; a mixture of fragmented (arrows) and condensed nuclei was found after STS treatment. Bars

represent 10  $\mu$ m. **b** Quantitative analysis of changes in nuclear morphology in transfected cells after treatment with H<sub>2</sub>O<sub>2</sub> or STS. The term “modified” here encompasses nuclei scored as condensed or fragmented. Note that the prevalence of modified nuclear morphology after STS treatment observed here at 24 h (~50%) is close to that previously observed [26]. Black bars, nRNA; white bars, siAtg7. For H<sub>2</sub>O<sub>2</sub>, siAtg7 exerted a significant effect relative to nRNA ( $P < 0.0001$ ), and asterisk indicates time point where there was a significant difference (\* $P < 0.01$ )

#### Caspase-independent cell death following H<sub>2</sub>O<sub>2</sub> insult requires autophagic machinery in C57/Black 6 J cortical neurons

Acute oxidative stress, such as that following ischemic reperfusion injury during stroke can invoke a necrotic-like cell death that is devoid of caspase activity at the core or center of infarction [23, 24, 42]. We have previously shown that following acute H<sub>2</sub>O<sub>2</sub> insult, cortical neurons from C57 Black/6 J mice undergo programmed necrosis (PCD-type III) that is independent of effector caspase activity (specifically caspase-3 and caspase-7) [26]. Here we show that the lack of caspase-3 and caspase-7 activity is the result of these caspases not being cleaved following H<sub>2</sub>O<sub>2</sub> treatment. In non-neuronal cells the lack of caspase activity following oxidative stress has been attributed to oxidation of the thiol group within the active cysteine [43, 44]. However, the lack of cleavage of procaspase-3 and procaspase-7 following H<sub>2</sub>O<sub>2</sub> treatment suggests that the absence of caspase-3 and caspase-7 activity is not due to

oxidation of the active cysteine, but results from a defect further upstream in the cell death pathway. One possibility is that H<sub>2</sub>O<sub>2</sub> is indirectly blocking caspase-3 and caspase-7 activation by inducing iron-mediated inhibition of procaspase-9 [45], or depletion of ATP required for proteolytic activation of caspase-9 [46]. We show that caspase-9 is active following STS, but not H<sub>2</sub>O<sub>2</sub> insult, which probably explains the lack of activity of downstream effector caspase-3 and caspase-7 under oxidative stress.

Minimal caspase activity following H<sub>2</sub>O<sub>2</sub> treatment alludes to an alternative cell death pathway other than apoptosis under these conditions (c.f. [31]). Certainly, evidence exists for oxidative stress inducing autophagic cell death in transformed and cancer cell lines [47, 48]. We established that following H<sub>2</sub>O<sub>2</sub> insult, autophagic activity is elevated as determined by monitoring the formation of autophagic vesicles incorporating GFP-LC3. This result could be due to inhibition of the cysteine protease Atg4, which would promote lipidation of LC3 [49]. Specifically, the Cys77 residue of Atg4 has been shown to be a direct

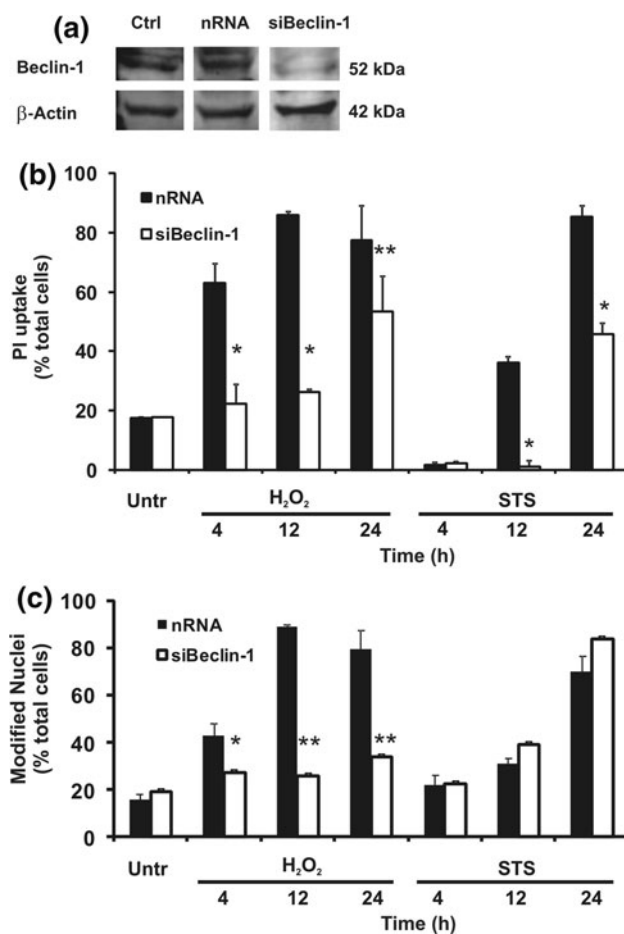


**Fig. 8** Cell death and changes in nuclear morphology in  $H_2O_2$ -treated and STS-treated primary cortical neurons transfected with nRNA and siBeclin 1. **a** Western immunoblots of Beclin 1 in cell lysates;  $\beta$ -actin is shown as loading control. Lanes indicate untransfected control (Ctrl), and cells transfected with nRNA or siBeclin 1. Sizes of proteins visualized (kDa) are indicated at right. Representative gel shown here indicates >80% suppression of Beclin 1 expression by siBeclin 1. **b** Quantitative analysis of PI uptake in transfected cells after treatment with  $H_2O_2$  or STS. Other indications are as for Fig. 6. **c** Quantitative analysis of changes in nuclear morphology in transfected cells after treatment with  $H_2O_2$  or STS. For **b**, **c**, black bars, nRNA; white bars, siBeclin 1. Results shown here report triplicate analyses within a single experiment. Due to the variation in Beclin 1 suppression achieved between experiments (see text), similar data obtained from three replicate experiments were not combined for quantification here. Other indications are as for Fig. 7. Asterisks indicate time points where there was a significant difference between nRNA and siBeclin 1 populations (**b**, \* $P < 0.001$ , \*\* $P < 0.01$ ; **c**, \* $P < 0.05$ , \*\* $P < 0.001$ )

target for oxidation by  $H_2O_2$  resulting in the inhibition of its protease activity.

Formation of autophagic vesicles incorporating GFP-LC3 was blocked by the autophagic inhibitor 3-MA. Furthermore, 3-MA also inhibited  $H_2O_2$ -induced cell death, suggesting PCD-type II occurs under these conditions. These data concur with similar studies recently undertaken on cerebellar granular neurons [50]. We confirmed the

involvement of autophagy in neuronal cell death by inhibiting cell death through the knockdown of both Beclin 1 and Atg7. We conclude that autophagy, or at least a component of the autophagic process, has a role in neuronal cell death under oxidative stress.

Elevation of autophagic activity under stress does not always result in cell death

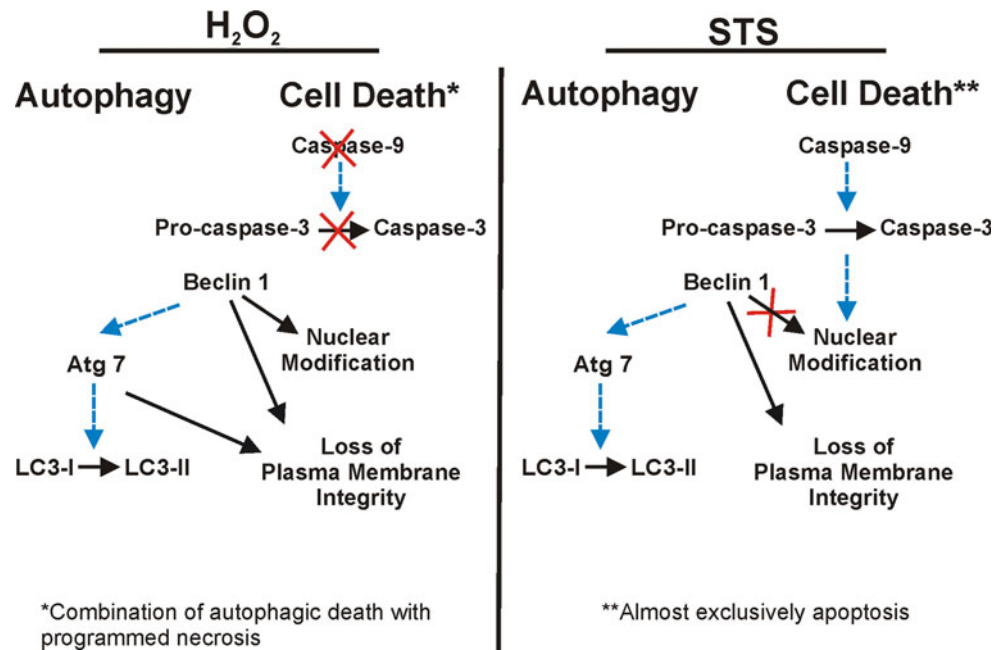
Autophagic activity was also elevated following STS treatment, but only after 24 h. Formation of autophagic vesicles was inhibited by pre-treatment with 3-MA. However, unlike in  $H_2O_2$ -treated neurons, 3-MA did not inhibit cell death after STS treatment. Knockdown of Atg7 also did not inhibit cell death. While it is evident that autophagic activity is amplified in STS-treated cells, it apparently has no role in cell death. Together, these observations raise the possibility that under these conditions autophagy is acting as a protective mechanism in an attempt to rescue neurons from death. Similar scenarios have been reported in neurons whereby misfolded proteins are cleared by the autophagy process [51]. Our findings show that for STS, caspase-3 is cleaved, a hallmark of classical neuronal apoptosis. However, caspase-7 was not activated. While caspase-7 has been shown to have a role in neuronal apoptosis in caspase-3-null mice [52], it is most likely not required when caspase-3 is available to act as the primary effector caspase. Our findings indicate that under conditions that are favorable for induction of apoptosis, such as with STS treatment, these cortical neurons do not invoke PCD-type II.

#### Dependence of PCD-type II on Atg7

Atg7 has generally been considered an essential component of the autophagy pathway in mammals. Atg7 is responsible for activating LC3-I and Atg12 during early formation of the isolation membrane or phagophore during macroautophagy [36]. Our findings showed that knockdown of Atg7 in cortical neurons blocked PCD-type-II following  $H_2O_2$  treatment, suggesting Atg7 has a critical role in the activation of autophagic cell death. Recently, however, an alternative autophagy pathway has been reported that does not require Atg5 or Atg7 for activation in non-neuronal mammalian cells [53]. Moreover, this alternate pathway did not involve the conversion of LC3-I to LC3-II for autophagosome formation. Atg5/Atg7-independent autophagy is thought to act under certain stressors and in different cell types, although the teleology of this alternate form of autophagy remains unclear. Evidently the autophagy we observed under  $H_2O_2$  insult was the more canonical form that is dependent on Atg7. It is worth noting that while STS-induced cell death could not be inhibited by Atg7



**Fig. 9** Schematic representation of autophagic and cell death events in primary cortical neurons treated with  $H_2O_2$  and STS. *Solid arrows* represent events that have been empirically defined in the present work. *X (red)* indicates steps that are not invoked under indicated treatment. *Dashed arrows (blue)* represent events that are known to occur in these types of treated cells, as demonstrated by other studies (references cited in text). Programmed necrosis, as mentioned under the left panel ( $H_2O_2$ ), was previously characterized in these neurons [26]



knockdown, evidence of LC3-II formation and the inhibition of puncta formed by GFP-LC3 with 3-MA indicates that the canonical pathway of macroautophagy was also being invoked following STS treatment.

#### Dual roles for Beclin 1 in neuronal cell death

The autophagy protein Beclin 1 has been implicated as an intermediary protein between apoptosis and autophagy because of its BH3-like domain [38]. In autophagy, Beclin 1 forms part of a complex that is essential for formation of the autophagosomal membrane [1]. Beclin 1 has also been shown to interact with Bcl-X<sub>L</sub> [38], although the exact teleology of this interaction remains unclear. Caspase-mediated cleavage of Beclin 1 has also been reported to amplify mitochondrion-mediated apoptosis [41]. In our work we knocked down Beclin 1 in an attempt to establish whether this protein was essential for PCD-type II.

In  $H_2O_2$ -treated neurons, Beclin 1 knockdown prevented changes in nuclear morphology and cell death. This finding is consistent with the view that autophagy directly contributes to cell death (PCD-type II). We have previously shown that redistribution of Endo G from mitochondria is an essential component of programmed necrosis in cortical neurons treated with  $H_2O_2$  [26]. Thus, a tentative conclusion might be that, under  $H_2O_2$  treatment, Beclin 1 may act as a key mediator between PCD-type II and PCD-type III, acting upstream of Atg7 and possibly Endo G, but this remains to be verified. However, in the case of STS, we showed that PCD-type II is not invoked (on the basis of Atg7 suppression and 3-MA treatment having little or no effect on cell death; see Fig. 9), yet Beclin 1 knockdown

inhibited cell death. Given that we have previously established [26] that STS induces apoptosis in these neurons, this result might suggest that Beclin 1 is acting in PCD-type I, at least in part. Nevertheless, in neurons treated with STS, changes in nuclear morphology occurred in spite of Beclin 1 suppression (as represented in Fig. 9). While Beclin 1 suppression blocked cell death (monitored by PI uptake) at early time points, by 24 h 40% of cells had died, indicating that cell death may not have been completely blocked but rather delayed. Hence, it is possible that Beclin 1 may be acting here in an auxiliary capacity promoting PCD-type I. In this context, caspase-mediated cleavage of Beclin 1 has recently been reported by others to enhance apoptosis [41]. However, Beclin-1 was not found to be cleaved in these neurons after STS treatment (data not shown). While caspase activity has been reported here, only a low number of neurons were scored positive for caspase-9 and -3 activity [26] relative to the total number of dead cells after 24 h. Thus, it is possible that another caspase-independent pathway to cell death may be operative within a subpopulation of STS-treated neurons [54], without involvement of Beclin 1. Overall, the differential involvement of Beclin 1 and Atg7 highlights the complexity of neuronal cell death and the significance of interaction between the different types of cell death.

#### Relationship between PCD-type II and other PCD pathways

Cross-talk has previously been reported to exist between apoptosis and autophagy [39, 55]. This apparently paradoxical link brings about tension in cellular decisions



leading either to life or death. However, it is now apparent that cross-talk between cell death pathways may be an essential part of cellular termination if one pathway is impeded. In the cortical neurons studied here, exposure to  $H_2O_2$  appears to block the activation of caspases, essentially disrupting recruitment of the classical apoptotic signaling pathway. Hence, cells must invoke an alternative cell death pathway, such as PCD-type II.

Our system is complex in yet another sense, as we have previously shown that programmed necrosis (PCD-type III) occurs following  $H_2O_2$  insult. Thus, we now suggest the possible existence of cross-talk between PCD-type II and PCD-type III, in line with the more general concept of cross-talk between cell death programs such as that which is thought to exist between PCD-type I and PCD-type II [39, 56–58]. Recently it has been reported that autophagy-dependent necroptosis (a subtype of programmed necrosis [59]) occurs in childhood acute lymphoblastic leukemia cells to overcome glucocorticoid resistance [60]. Thus, a similar type of scenario may be manifested in these cortical neurons in response to oxidative stress. However, we noted that while knockdown of Atg7 blocked cell death, it failed to impact upon changes in nuclear morphology associated with cell death. This observation suggests that interdependence may exist between PCD-type II and PCD-type III under  $H_2O_2$  insult, where each of these pathways is responsible for invoking certain cellular characteristics independently.

#### Perspectives on autophagic cell death in neurons

Acute oxidative stress has long been recognized as an initiator of caspase-independent cell death, previously thought of as unregulated necrosis. In pathological settings such as stroke, arresting cell death at the center of infarction, where the most severe neuronal damage occurs, has posed the greatest challenge. Current thinking considers that cell death at the “necrotic core” may not necessarily be unregulated necrosis. Further detailed investigation is warranted to establish whether the cell death outcome at the core of infarction is, in fact, unregulated necrosis or whether it encompasses other types of cell death, including PCD-type II and -type III. Indeed, there is an emergent literature showing that autophagic mechanisms contribute to hypoxic-ischaemic injury [42].

The present study has demonstrated that under oxidative stress, generated by  $H_2O_2$ , invokes a cell death that is dependent on autophagy in the absence of caspase activation. Furthermore, our findings suggest that autophagy acts as an alternative form of death to apoptosis and that it is capable of interacting with other types of cell death such as programmed necrosis. These issues and the interdependence of cell death pathways require considerable attention

and are directly relevant to the pharmacotherapy of neuropathologies [22].

**Acknowledgments** We thank Ms. Sue Ekkel for technical assistance with Western immunoblotting and Dr. Danielle Smith for technical advice. This work was supported by the National Health and Medical Research Council (Australia), of which Philip M. Beart is a Research Fellow. Phillip Nagley and Rodney J. Devenish are also supported by the Australian Research Council.

#### References

1. Jaeger PA, Wyss-Coray T (2009) All-you-can-eat: autophagy in neurodegeneration and neuroprotection. *Mol Neurodegener* 4:16
2. Boland B, Nixon RA (2006) Neuronal macroautophagy: from development to degeneration. *Mol Aspects Med* 27:503–519
3. He C, Klionsky DJ (2009) Regulation mechanisms and signaling pathways of autophagy. *Annu Rev Genet* 43:67–93
4. Rubinsztein DC, DiFiglia M, Heintz N, Nixon RA, Qin ZH, Ravikumar B, Stefanis L, Tolkovsky A (2005) Autophagy and its possible roles in nervous system diseases, damage and repair. *Autophagy* 1:11–22
5. Clark RS, Bayir H, Chu CT, Alber SM, Kochanek PM, Watkins SC (2008) Autophagy is increased in mice after traumatic brain injury and is detectable in human brain after trauma and critical illness. *Autophagy* 4:88–90
6. Diskin T, Tal-Or P, Erlich S, Mizrachy L, Alexandrovich A, Shohami E, Pinkas-Kramarski R (2005) Closed head injury induces upregulation of Beclin 1 at the cortical site of injury. *J Neurotrauma* 22:750–762
7. Lai Y, Hickey RW, Chen Y, Bayir H, Sullivan ML, Chu CT, Kochanek PM, Dixon CE, Jenkins LW, Graham SH, Watkins SC, Clark RS (2008) Autophagy is increased after traumatic brain injury in mice and is partially inhibited by the antioxidant gamma-glutamylcysteinyl ethyl ester. *J Cereb Blood Flow Metab* 28:540–550
8. Yamashima T, Oikawa S (2009) The role of lysosomal rupture in neuronal death. *Prog Neurobiol* 89:343–358
9. Chu CT, Plowey ED, Dagda RK, Hickey RW, Cherra SJ 3rd, Clark RS (2009) Autophagy in neurite injury and neurodegeneration: in vitro and in vivo models. *Methods Enzymol* 453:217–249
10. Zhu C, Wang X, Xu F, Bahr BA, Shibata M, Uchiyama Y, Hagberg H, Blomgren K (2005) The influence of age on apoptotic and other mechanisms of cell death after cerebral hypoxia-ischemia. *Cell Death Differ* 12:162–176
11. Clarke PG (1990) Developmental cell death: morphological diversity and multiple mechanisms. *Anat Embryol (Berl)* 181:195–213
12. Kroemer G, Galluzzi L, Vandenabeele P, Abrams J, Alnemri ES, Baehrecke EH, Blagosklonny MV, El-Deiry WS, Golstein P, Green DR, Hengartner M, Knight RA, Kumar S, Lipton SA, Malorni W, Nunez G, Peter ME, Tschopp J, Yuan J, Piacentini M, Zhivotovsky B, Melino G (2009) Classification of cell death: recommendations of the Nomenclature Committee on Cell Death 2009. *Cell Death Differ* 16:3–11
13. Chakrabarti L, Eng J, Ivanov N, Garden GA, La Spada AR (2009) Autophagy activation and enhanced mitophagy characterize the Purkinje cells of pcd mice prior to neuronal death. *Mol Brain* 2:24
14. Baba H, Sakurai M, Abe K, Tominaga R (2009) Autophagy-mediated stress response in motor neuron after transient ischemia in rabbits. *J Vasc Surg* 50:381–387
15. Lang-Rollin IC, Rideout HJ, Noticewala M, Stefanis L (2003) Mechanisms of caspase-independent neuronal death: energy depletion and free radical generation. *J Neurosci* 23:11015–11025

16. Xue L, Fletcher GC, Tolkovsky AM (1999) Autophagy is activated by apoptotic signalling in sympathetic neurons: an alternative mechanism of death execution. *Mol Cell Neurosci* 14:180–198
17. Halliwell B (2006) Oxidative stress and neurodegeneration: where are we now? *J Neurochem* 97:1634–1658
18. Jenner P (2007) Oxidative stress and Parkinson's disease. *Handb Clin Neurol* 83:507–520
19. Niizuma K, Endo H, Chan PH (2009) Oxidative stress and mitochondrial dysfunction as determinants of ischemic neuronal death and survival. *J Neurochem* 109(Suppl 1):133–138
20. Higgins GC, Beart PM, Shin YS, Chen MJ, Cheung NS, Nagley P (2010) Oxidative stress: emerging mitochondrial and cellular themes and variations in neuronal injury. *J Alzheimers Dis* 20(Suppl 2):S453–S473
21. Nakka VP, Gusain A, Mehta SL, Raghuram R (2008) Molecular mechanisms of apoptosis in cerebral ischemia: multiple neuro-protective opportunities. *Mol Neurobiol* 37:7–38
22. Degterev A, Yuan J (2008) Expansion and evolution of cell death programmes. *Nat Rev Mol Cell Biol* 9:378–390
23. Blomgren K, Leist M, Groc L (2007) Pathological apoptosis in the developing brain. *Apoptosis* 12:993–1010
24. Gill MB, Perez-Polo JR (2008) Hypoxia ischemia-mediated cell death in neonatal rat brain. *Neurochem Res* 33:2379–2389
25. Degterev A, Huang Z, Boyce M, Li Y, Jagtap P, Mizushima N, Cuny GD, Mitchison TJ, Moskowicz MA, Yuan J (2005) Chemical inhibitor of nonapoptotic cell death with therapeutic potential for ischemic brain injury. *Nat Chem Biol* 1:112–119
26. Higgins GC, Beart PM, Nagley P (2009) Oxidative stress triggers neuronal caspase-independent death: endonuclease G involvement in programmed cell death-type III. *Cell Mol Life Sci* 66:2773–2787
27. Koh JY, Wie MB, Gwag BJ, Sensi SL, Canzoniero LM, Demaro J, Csernansky C, Choi DW (1995) Staurosporine-induced neuronal apoptosis. *Exp Neurol* 135:153–159
28. Cheung NS, Beart PM, Pascoe CJ, John CA, Bernard O (2000) Human Bcl-2 protects against AMPA receptor-mediated apoptosis. *J Neurochem* 74:1613–1620
29. Beart PM, Lim ML, Chen B, Diwakarla S, Mercer LD, Cheung NS, Nagley P (2007) Hierarchical recruitment by AMPA but not staurosporine of pro-apoptotic mitochondrial signaling in cultured cortical neurons: evidence for caspase-dependent/independent cross-talk. *J Neurochem* 103:2408–2427
30. Kabeya Y, Mizushima N, Ueno T, Yamamoto A, Kirisako T, Noda T, Kominami E, Ohsumi Y, Yoshimori T (2000) LC3, a mammalian homologue of yeast Apg8p, is localized in autophagosome membranes after processing. *EMBO J* 19:5720–5728
31. Diwakarla S, Nagley P, Hughes ML, Chen B, Beart PM (2009) Differential insult-dependent recruitment of the intrinsic mitochondrial pathway during neuronal programmed cell death. *Cell Mol Life Sci* 66:156–172
32. Lim ML, Chen B, Beart PM, Nagley P (2006) Relative timing of redistribution of cytochrome c and Smac/DIABLO from mitochondria during apoptosis assessed by double immunocytochemistry on mammalian cells. *Exp Cell Res* 312:1174–1184
33. Renatus M, Stennicke HR, Scott FL, Liddington RC, Salvesen GS (2001) Dimer formation drives the activation of the cell death protease caspase 9. *Proc Natl Acad Sci USA* 98:14250–14255
34. Tanida I, Ueno T, Kominami E (2004) LC3 conjugation system in mammalian autophagy. *Int J Biochem Cell Biol* 36:2503–2518
35. Klionsky DJ, Abeliovich H, Agostinis P, Agrawal DK, Aliev G, Askew DS, Baba M, Baehrecke EH, Bahr BA, Ballabio A, Bamber BA, Bassham DC, Bergamini E, Bi X, Biard-Piechaczyk M, Blum JS, Breiden DE, Brodsky JL, Brumell JH, Brunk UT, Bursch W, Camougrand N, Cebollero E, Cecconi F, Chen Y, Chin LS, Choi A, Chu CT, Chung J, Clarke PG, Clark RS, Clarke SG, Clave C, Cleveland JL, Codogno P, Colombo MI, Coto-Montes A, Cregg JM, Cuervo AM, Debnath J, Demarchi F, Dennis PB, Dennis PA, Deretic V, Devenish RJ, Di Sano F, Dice JF, Difiglia M, Dinesh-Kumar S, Distelhorst CW, Djavaheri-Mergny M, Dorsey FC, Droge W, Dron M, Dunn WA Jr, Duszenko M, Eissa NT, Elazar Z, Esclatine A, Eskelinen EL, Fesus L, Finley KD, Fuentes JM, Fueyo J, Fujisaki K, Galliot B, Gao FB, Gewirtz DA, Gibson SB, Gohla A, Goldberg AL, Gonzalez R, Gonzalez-Estevez C, Gorski S, Gottlieb RA, Haussinger D, He YW, Heidenreich K, Hill JA, Hoyer-Hansen M, Hu X, Huang WP, Iwasaki A, Jaattela M, Jackson WT, Jiang X, Jin S, Johansen T, Jung JU, Kadowaki M, Kang C, Kelekar A, Kessel DH, Kiel JA, Kim HP, Kimchi A, Kinsella TJ, Kiselyov K, Kitamoto K, Knecht E, Komatsu M, Kominami E, Kondo S, Kovacs AL, Kroemer G, Kuan CY, Kumar R, Kundu M, Landry J, Laporte M, Le W, Lei HY, Lenardo MJ, Levine B, Lieberman A, Lim KL, Lin FC, Liou W, Liu LF, Lopez-Berestein G, Lopez-Otin C, Lu B, Macleod KF, Malorni W, Martinet W, Matsuoka K, Mautner J, Meijer AJ, Melendez A, Michels P, Miotto G, Mistiaen WP, Mizushima N, Mograbi B, Monastyrskaya I, Moore MN, Moreira PI, Moriyasu Y, Motyl T, Munz C, Murphy LO, Naqvi NI, Neufeld TP, Nishino I, Nixon RA, Noda T, Numborg B, Ogawa M, Oleinick NL, Olsen LJ, Ozpolat B, Paglin S, Palmer GE, Papassideri I, Parkes M, Perlmutter DH, Perry G, Piacentini M, Pinkas-Kramarski R, Prescott M, Proikas-Cezanne T, Raben N, Rami A, Reggiori F, Rohrer B, Rubinsztein DC, Ryan KM, Sadoshima J, Sakagami H, Sakai Y, Sandri M, Sasakawa C, Sass M, Schneider C, Seglen PO, Seleverstov O, Settlement J, Shacka JJ, Shapiro IM, Sibirny A, Silva-Zacarin EC, Simon HU, Simone C, Simonsen A, Smith MA, Spaniel-Borowski K, Srinivas V, Steeves M, Stenmark H, Stromhaug PE, Subauste CS, Sugimoto S, Sulzer D, Suzuki T, Swanson MS, Tabas I, Takeshita F, Talbot NJ, Talloczy Z, Tanaka K, Tanaka K, Tanida I, Taylor GS, Taylor JP, Terman A, Tettamanti G, Thompson CB, Thumm M, Tolkovsky AM, Tooze SA, Truant R, Tumanovska LV, Uchiyama Y, Ueno T, Uzcategui NL, van der Klei I, Vaquero EC, Vellai T, Vogel MW, Wang HG, Webster P, Wiley JW, Xi Z, Xiao G, Yahalom J, Yang JM, Yap G, Yin XM, Yoshimori T, Yu L, Yue Z, Yuzaki M, Zabirnyk O, Zheng X, Zhu X, Deter RL (2008) Guidelines for the use and interpretation of assays for monitoring autophagy in higher eukaryotes. *Autophagy* 4:151–175
36. Mehrpour M, Esclatine A, Beau I, Codogno P (2010) Autophagy in health and disease. 1. Regulation and significance of autophagy: an overview. *Am J Physiol Cell Physiol* 298:C776–C785
37. Barth S, Glick D, Macleod KF (2010) Autophagy: assays and artifacts. *J Pathol* 221:117–124
38. Maiuri MC, Le Toumelin G, Criollo A, Rain JC, Gautier F, Juin P, Tasdemir E, Pierron G, Troulinaki K, Tavernarakis N, Hickman JA, Geneste O, Kroemer G (2007) Functional and physical interaction between Bcl-X(L) and a BH3-like domain in Beclin-1. *EMBO J* 26:2527–2539
39. Maiuri MC, Criollo A, Kroemer G (2010) Crosstalk between apoptosis and autophagy within the Beclin 1 interactome. *EMBO J* 29:515–516
40. Garcia-Arencibia M, Hochfeld WE, Toh PP, Rubinsztein DC (2010) Autophagy, a guardian against neurodegeneration. *Semin Cell Dev Biol* 21:691–698
41. Wirawan E, Vande Walle L, Kersse K, Cornelis S, Claerhout S, Vanoverberghe I, Roelandt R, De Rycke R, Verspurten J, Declercq W, Agostinis P, Vanden Berghe T, Lippens S, Vandenabeele P (2010) Caspase-mediated cleavage of Beclin-1 inactivates Beclin-1 induced autophagy and enhances apoptosis by promoting the release of proapoptotic factors from mitochondria. *Cell Death Dis* 1:e18
42. Nagley P, Higgins GC, Atkin JD, Beart PM (2010) Multifaceted deaths orchestrated by mitochondria in neurones. *Biochim Biophys Acta* 1802:167–185

43. Carmody RJ, Cotter TG (2000) Oxidative stress induces caspase-independent retinal apoptosis in vitro. *Cell Death Differ* 7:282–291
44. Haendeler J, Weiland U, Zeiher AM, Dimmeler S (1997) Effects of redox-related congeners of NO on apoptosis and caspase-3 activity. *Nitric Oxide* 1:282–293
45. Barbouti A, Amorgianiotis C, Kolettas E, Kanavaros P, Galaris D (2007) Hydrogen peroxide inhibits caspase-dependent apoptosis by inactivating procaspase-9 in an iron-dependent manner. *Free Radic Biol Med* 43:1377–1387
46. Lee YJ, Shacter E (2000) Hydrogen peroxide inhibits activation, not activity, of cellular caspase-3 in vivo. *Free Radic Biol Med* 29:684–692
47. Chen Y, McMillan-Ward E, Kong J, Israels SJ, Gibson SB (2007) Mitochondrial electron-transport-chain inhibitors of complexes I and II induce autophagic cell death mediated by reactive oxygen species. *J Cell Sci* 120:4155–4166
48. Chen Y, McMillan-Ward E, Kong J, Israels SJ, Gibson SB (2008) Oxidative stress induces autophagic cell death independent of apoptosis in transformed and cancer cells. *Cell Death Differ* 15:171–182
49. Scherz-Shouval R, Shvets E, Fass E, Shorer H, Gil L, Elazar Z (2007) Reactive oxygen species are essential for autophagy and specifically regulate the activity of Atg4. *EMBO J* 26:1749–1760
50. Maycotte P, Guemez-Gamboa A, Moran J (2010) Apoptosis and autophagy in rat cerebellar granule neuron death: role of reactive oxygen species. *J Neurosci Res* 88:73–85
51. Klionsky DJ (2006) Neurodegeneration: good riddance to bad rubbish. *Nature* 441:819–820
52. Houde C, Banks KG, Coulombe N, Rasper D, Grimm E, Roy S, Simpson EM, Nicholson DW (2004) Caspase-7 expanded function and intrinsic expression level underlies strain-specific brain phenotype of caspase-3-null mice. *J Neurosci* 24:9977–9984
53. Nishida Y, Arakawa S, Fujitani K, Yamaguchi H, Mizuta T, Kanaseki T, Komatsu M, Otsu K, Tsujimoto Y, Shimizu S (2009) Discovery of Atg5/Atg7-independent alternative macroautophagy. *Nature* 461:654–658
54. Diwakarla S, Mercer LD, Kardashsyan L, Chu PW, Shin YS, Lau CL, Hughes ML, Nagley P, Beart PM (2009) GABAergic striatal neurons exhibit caspase-independent, mitochondrially mediated programmed cell death. *J Neurochem* 109(Suppl 1):198–206
55. Djavaheri-Mergny M, Maiuri MC, Kroemer G (2010) Cross talk between apoptosis and autophagy by caspase-mediated cleavage of Beclin 1. *Oncogene* 29:1717–1719
56. Maiuri MC, Criollo A, Tasdemir E, Vicencio JM, Tajeddine N, Hickman JA, Geneste O, Kroemer G (2007) BH3-only proteins and BH3 mimetics induce autophagy by competitively disrupting the interaction between Beclin 1 and Bcl-2/Bcl-X(L). *Autophagy* 3:374–376
57. Pattingre S, Tassa A, Qu X, Garuti R, Liang XH, Mizushima N, Packer M, Schneider MD, Levine B (2005) Bcl-2 antiapoptotic proteins inhibit Beclin 1-dependent autophagy. *Cell* 122:927–939
58. Yousefi S, Perozzo R, Schmid I, Ziemiecki A, Schaffner T, Scapozza L, Brunner T, Simon HU (2006) Calpain-mediated cleavage of Atg5 switches autophagy to apoptosis. *Nat Cell Biol* 8:1124–1132
59. Galluzzi L, Kroemer G (2008) Necroptosis: a specialized pathway of programmed necrosis. *Cell* 135:1161–1163
60. Bonapace L, Bornhauser BC, Schmitz M, Cario G, Ziegler U, Niggli FK, Schafer BW, Schrappe M, Stanulla M, Bourquin JP (2010) Induction of autophagy-dependent necroptosis is required for childhood acute lymphoblastic leukemia cells to overcome glucocorticoid resistance. *J Clin Invest* 120:1310–1323